THEORETICA CHIMICA ACTA
Theoret. Chim. Acta (Berl.) 61, 203–226 (1982)

A Constant Denominator Perturbation Theory for Molecular Energy

John M. Cullen* and Michael C. Zerner

The Guelph-Waterloo Centre for Graduate Work in Chemistry, Department of Chemistry, University of Guelph, Guelph, Ontario, Canada N1G 2W1

A "constant denominator" perturbation theory is developed based on a zeroth order Hamiltonian characterized by degenerate subsets of orbitals. Such a formulation allows for a decoupling of the numerators of the perturbation sequence, allowing for much more rapid evaluation of the resultant sums. For example, the full fourth order theory can be evaluated as an N^6 step rather than N^7, where N is proportional to the basis set.
Although the theory is general, a constant denominator is chosen for this study as the difference between the average occupied and average virtual orbital energies scaled so that the first order wavefunction yields the lowest possible variational bound. The third order correction then appears naturally as a scaled Langhoff-Davidson correction. The full fourth order with this partitioning is developed. Results are presented within the localized bond model utilizing both the Pariser–Parr–Pople and CNDO/2 model Hamiltonians. The second order theory presents a useful bound, usually containing a good deal of the basis set correlation. In all cases examined the fourth order theory shows remarkable stability, even in those cases in which the Nesbet–Epstein partitioning seems poorly convergent, and the Moller–Plesset theory uncertain.

Key words: Perturbation theory – Fourth order perturbation theory – Electron correlation – Constant denominator perturbation theory.

* *Present address*: Environmental Contaminants Division, Canada Centre for Inland Waters, P.O. Box 5050, Burlington, Ontario L7R 4A6, Canada

MS 231 0040-5744/82/0061/0203/$04.80

1. Introduction

Perturbation treatments are computationally the fastest of all known methods for estimating electron correlation. The work of Bartlett and coworkers [1–5] and others [6–8] have demonstrated that, at least for small molecules, a perturbation expansion carried out to fourth order is sufficient to give results within kilocalorie accuracy of experiment. However, an exact fourth order treatment may not be practical for *ab initio* methods since the triple excitations which occur require a lengthy N^7 step, where N is the number of molecular orbitals. In this paper we present an alternative partitioning of the Hamiltonian different from the usual Moller–Plesset [9] or Nesbet–Epstein [10] types used in perturbation theory which allows for the calculation of the triple excitations in an N^6

Table 1. Comparison of canonical (Hartree–Fock) orbital energies and the localized orbital energies[a]

Molecule	Canonical orbital energies	Localized orbital energies	Molecule	Canonical orbital energies	Localized orbital energies
CH_4	0.3306	0.3202	C_2H_6	−0.8658	−0.8673
	0.3306	0.3202		−0.8659	−0.8673
	0.3306	0.3202		−1.0740	−0.8673
	0.3102	0.3202		−1.4812	−0.9431
	−0.7256	0.8666			
	−0.7256	0.8666	CH_3CN	0.5852	0.5105
	−0.7256	0.8666		0.3538	0.3956
	−1.2710	0.8666		0.3536	0.2995
				0.3461	0.2995
C_2H_2	0.5758	0.5015		0.2806	0.2995
	0.3455	0.3183		0.2157	0.2510
	0.2729	0.3184		0.2156	0.2510
	0.2729	0.2531		−0.5841	−0.6693
	0.2557	0.2531		−0.5841	−0.6693
	−0.6428	−0.6627		−0.6353	−0.7675
	−0.6428	−0.6627		−0.8425	−0.8867
	−0.7572	−0.9263		−0.8544	−0.8867
	−0.9752	−0.9263		−0.8545	−0.8867
	−1.3548	−1.2554		−1.3442	−1.0622
				−1.5016	−1.3296
C_2H_6	0.3952	0.3845			
	0.3740	0.3200			
	0.3738	0.3200			
	0.3157	0.3200			
	0.2967	0.3200			
	0.2900	0.3200			
	0.2897	0.3200			
	−0.6008	−0.8673			
	−0.6009	−0.8763			
	−0.6688	−0.8763			

[a] All energies given in atomic units

step. Instead of using a set of canonical SCF orbitals, localized orbitals are chosen to describe the system. Although numerous techniques [11] exist for transforming into a set of localized orbitals, in practice all lead to essentially the same result. That is, a set of well localized orbitals is found for the atomic cores, molecular bonds, and lone pairs in agreement with the usual chemical description of electron pairs. The properties of localized orbitals such as their transferability and their better convergence rate in CI expansion compared to that found using a canonical set of molecular orbitals have been well documented [12–17]. Perhaps less well appreciated has been the observation that the sets of core, bonding and antibonding orbital energies are quasi-degenerate among themselves. In Table 1 are presented examples for CH_4, C_2H_2, C_2H_6 and CH_3CN for the semi-empirical CNDO/2 model where the localized orbitals ϕ_i and ϕ_{i^*} are simply chosen as linear and antilinear combinations of a hybridized set of primitive atomic orbitals χ_A and χ_B on centres A and B respectively. That is

$$\phi_i = \sin\alpha \cdot \chi_A + \cos\alpha \cdot \chi_B \tag{1a}$$

$$\phi_{i^*} = \cos\alpha \cdot \chi_A - \sin\alpha \cdot \chi_B \tag{1b}$$

where α is a "polarity parameter"; the case of $\alpha = 45°$ meaning no polarity of the bond. All this suggests a partitioning of H based on the average orbital energies of the respective sets. The resultant perturbation expansion then has denominators which are integral multiples of a small number of constants, the constants being simply the differences among the various average orbital energies.

In this paper we develop this constant denominator perturbation theory for the case of a minimum basis. Furthermore we assume that the core may be replaced with a suitable pseudo potential. However, the method can be easily generalized to cases where the core is explicitly considered and extensive basis sets used. We begin by briefly reviewing the conventional Moller–Plesset and Nesbet–Epstein partitionings of the Hamiltonian. The constant denominator partitioning is then derived. Although any constant denominator can be chosen, we choose to examine here the average orbital energies variationally modified so that the truncated perturbation expanded wave function will yield the lowest bound for the Rayleigh–Ritz optimization procedure

$$\frac{\langle\psi|H|\psi\rangle}{\langle\psi|\psi\rangle} \geq E. \tag{2}$$

Formulae are developed diagrammatically up to and including fourth order in the perturbation for the energy. The formal N^7 step found for contributions from triple excitations is shown to be reduced into steps which are at most N^6. As examples, results are presented calculated within the semi-empirical PPP [18] and CNDO/2 [19] model Hamiltonians

2. Partitioning of the Hamiltonian

One starts any perturbation treatment for the energy by partitioning the Hamiltonian, H, into a completely solvable zero order part, H_0, and a remainder

known as the perturbation, V

$$H = H_0 + V \tag{3a}$$

where

$$H_0|\Phi_i\rangle = \tilde{\varepsilon}_i|\Phi_i\rangle \qquad i = 0, 1, 2, \ldots . \tag{3b}$$

In addition, H_0 is usually chosen to be a one particle operator in order that the linked diagrammatic representation of the perturbation can be used

$$H_0 = \sum_{\alpha} u_\alpha(\vec{r}_\alpha) \tag{4a}$$

with

$$u_\alpha|\phi_\alpha\rangle = \varepsilon_\alpha|\phi_\alpha\rangle \tag{4b}$$

$$|\Phi_i\rangle = A \prod_{\alpha \varepsilon i} |\phi_\alpha\rangle \tag{4c}$$

$$\tilde{\varepsilon}_i = \prod_{\alpha \varepsilon i} \varepsilon_\alpha \tag{4d}$$

where A is the antisymmetrizer and u_α is a single particle operator. In the case of Moller–Plesset partitioning, H_0 is chosen to be the Fock operator and therefore due to Brillouin's theorem the perturbation V contains only Coulombic bielectronic repulsion and exchange integrals. In contrast, the Nesbet–Epstein partitioning is based on the matrix representation of the Schrödinger equation

$$H\psi = E\psi \tag{5}$$

H_0, the zero order Hamiltonian is chosen simply as the diagonal of H with the remaining off diagonal matrix forming the perturbation V. In the case of spin adapted configurations, ψ, one obtains a corresponding spin adapted Nesbet–Epstein partitioning. Calculations [20] show that this spin adapted partitioning is more convergent than the ordinary expansion over determinants. However, since the denominators in the perturbation expansion now are coupled by bielectronic matrix elements, they cannot be factored to yield a linked diagrammatic representation. In order to achieve the Nesbet–Epstein result from a diagrammatic formulation of the perturbation one must first start from a Moller–Plesset reference, generate the necessary diagrams and then group into geometric sums classes of diagrams known as ladder diagrams. The geometric sums are then replaced by inserting bielectronic interactions into the denominators of the leading terms. This is essentially the procedure that Kelly [23] used with great success for atomic systems. However Bartlett and Shavitt [24, 25] found in the case of the linearized CPMET model [26] that Nesbet–Epstein partitioning led to oscillatory behaviour and produced a slower convergence than that found for Moller–Plesset partitioning [22].

3. The Constant Denominator Partitioning

The quasi-degeneracies found among the sets of localized orbital energies allow for a consideration of a partitioning of H based on the average values of the respective sets. In the case of a minimum basis with a pseudo potential approximated core one has two sets, namely the bonding and antibonding orbitals $\{\phi_i\}$ and $\{\phi_{i^*}\}$ respectively. Therefore

$$H_0 = \bar{\varepsilon} \sum_i a_i \dagger a_i + \bar{\varepsilon}^* \sum_i a_{i^*}^{\dagger} a_{i^*} \tag{6}$$

$$V = H - H_0 \tag{7}$$

$$\bar{\varepsilon} = \frac{1}{N} \sum_{i=1}^{N} \varepsilon_i \tag{8}$$

$$\bar{\varepsilon}^* = \frac{1}{M} \sum_{i=1}^{M} \varepsilon_{i^*}. \tag{9}$$

The resulting denominators found in the perturbation expansion, as for example

$$\Delta\varepsilon_j^{i^*} = \varepsilon_j - \varepsilon_{i^*} \tag{10a}$$

$$\Delta\varepsilon_k^{i^* j^*} = \varepsilon_k + \varepsilon_l - \varepsilon_{i^*} - \varepsilon_{l^*} \tag{10b}$$

are reduced to integral factors of a constant denominator, ΔE, given by

$$\Delta\varepsilon = \bar{\varepsilon} - \bar{\varepsilon}^*. \tag{10c}$$

One can improve on the partitioning with very little additional computational effort by treating the constant denominator as a variational parameter, $\lambda\Delta\varepsilon$, with λ chosen to give the best trial wave function

$$|\psi_T\rangle = |\phi_0\rangle + \sum_{q=1}^{M} |\psi_q(\lambda)\rangle. \tag{11a}$$

Following the Rayleigh–Ritz variational principle, the resulting upper bound to the true ground state energy is given by

$$W = \sum_{pq=0}^{M} \frac{H_{p,q}}{1+S} \geq E \tag{11b}$$

with

$$H_{p,q} = \langle\psi_p|H|\psi_q\rangle \tag{11c}$$

$$S = \sum_{pq=1} S_{p,q} \tag{11d}$$

$$S_{p,q} = \langle\psi_p|\psi_q\rangle. \tag{11e}$$

The wave function corrections, $|\psi_q\rangle$, can be found from the perturbation equation

$$(H_0 - \tilde{\varepsilon}_0)|\psi_q\rangle + V|\psi_{q-1}\rangle = \sum_{r=1}^{q} E_r|\psi_{q-r}\rangle \tag{12a}$$

or in terms of matrix elements

$$T_{p,q} + V_{p,q-1} = \sum_{r=1}^{q} E_r S_{p,q-r} \tag{12b}$$

with

$$T_{p,q} = \langle \psi_p | H_0 - \tilde{\varepsilon}_0 | \psi_q \rangle \tag{12c}$$

$$V_{p,q} = \langle \psi_p | V | \psi_q \rangle. \tag{12d}$$

Therefore Eq. (11b) can be expanded as

$$W = \tilde{\varepsilon}_0 + \frac{\sum_{pq=0}^{M} T_{p,q} + \sum_{pq=0}^{M} V_{p,q-1} + \sum_{p=0}^{M} V_{pM}}{1+S}$$

$$= \tilde{\varepsilon}_0 + E_1 + \frac{\sum_{p=0}^{M} \sum_{q=2}^{M} \sum_{r=2}^{q} E_r S_{p,q-r} + \sum_{p=0}^{M} (V_{pM} - E_1 S_{pM})}{1+S} \tag{12e}$$

or substituting for V_{pM}, using Eq. (12b) yields

$$W = \tilde{\varepsilon}_0 + E_1 + \frac{\sum_{pq=0}^{M} \sum_{r=2}^{q} E_r S_{p,q-r} + \sum_{p=0}^{M} \sum_{r=2}^{M+1} E_r S_{p,M-r+1} - \sum_{p=0}^{M} T_{p,M+1}}{1+S}$$

$$= \tilde{\varepsilon}_0 + E_1 + \frac{\sum_{q=2}^{M+1} \sum_{r=2}^{q} \sum_{p=0}^{M} S_{p,q-r} - \sum_{p=1}^{M} T_{p,M+1}}{1+S}. \tag{12f}$$

By varying λ, the partitioning changes, producing a new set of perturbation energies $E_n(\lambda)$ and matrix elements $S_{p,q}(\lambda)$ and $T_{p,q}(\lambda)$. Noting that

$$E_2 = \frac{E_2}{(\lambda + (1-\lambda))} = \frac{E_2}{\lambda} \sum_{r=0}^{\infty} (-1)^r \left(\frac{1-\lambda}{\lambda}\right)^r \tag{13a}$$

$$E_3 = \frac{E_3}{(\lambda + (1-\lambda))^2} = \frac{E_3}{\lambda^2} \sum_{r=0}^{\infty} (-1)^r \left(\frac{1-\lambda}{\lambda}\right)^r (r+1) \tag{13b}$$

$$E_n = \frac{E_n}{(\lambda + (1-\lambda))^{n-1}} = \frac{E_n}{\lambda^{n-1}} \sum_{r=0}^{\infty} (-1)^r \left(\frac{1-\lambda}{\lambda}\right)^r \binom{r+n-2}{r} \tag{13c}$$

where the binomial coefficient $\binom{n}{m}$ is defined as

$$\binom{n}{m} = \frac{n!}{m!(n-m)!}. \tag{13d}$$

Regrouping terms, we obtain

$$E_2(\lambda) = \frac{E_2}{\lambda} \tag{14a}$$

$$E_3^{(3)}(\lambda)=\frac{E_3^{(3)}}{\lambda^2}-\frac{E_2^{(2)}}{\lambda^2}(1-\lambda) \tag{14b}$$

$$E_n(\lambda)=\frac{1}{\lambda^{n-1}}\sum_{i=0}^{n-2}E_{n-i}(-1)^r(1-\lambda)^r\binom{n-2}{r}. \tag{14c}$$

In a similar fashion

$$|\psi_p(\lambda)\rangle=\frac{1}{\lambda^p}\sum_{r=0}^{p-1}|\psi_{p-r}\rangle\binom{p-1}{r}(-1)^r(1-\lambda)^r \tag{15a}$$

from which is obtained expressions for the matrix elements $S_{p,q}(\lambda)$ and $T_{p,q}(\lambda)$.

$$S_{p,q}(\lambda)=\frac{1}{\lambda^{p+q}}\sum_{m=0}^{p-1}\sum_{n=0}^{q-1}\binom{p-1}{m}\binom{q-1}{n}(-1)^{m+n}(1-\lambda)^{m+n}S_{p-m,q-n} \tag{15b}$$

$$T_{p,q}(\lambda)=\frac{1}{\lambda^{p+q}}\sum_{m=0}^{p-1}\sum_{n=0}^{q-1}\binom{p-1}{m}\binom{q-1}{n}(-1)^{m+n}(1-\lambda)^{m+n}T_{p-m,q-n}. \tag{15c}$$

In the case of a perturbation expansion (11) carried out to first order Eq. (12f) simplifies to

$$\begin{aligned}W&=\tilde{\varepsilon}_0+E_1+\frac{E_2(\lambda)-T_{1,2}(\lambda)}{1+S(\lambda)}\\&=\tilde{\varepsilon}_0+E_1+\frac{E_2(\lambda)+E_3(\lambda)}{1+S(\lambda)}.\end{aligned} \tag{16a}$$

Substitution of relations (13) yields

$$W=\tilde{\varepsilon}_0+E_1+\frac{\frac{2E_2}{\lambda}+\frac{E_3}{\lambda^2}-\frac{E_2}{\lambda^2}}{1+\frac{S}{\lambda^2}}. \tag{17}$$

The solution to $\partial W/\partial\lambda=0$ is then given by

$$\lambda=\tfrac{1}{2}[(1-\gamma)+\sqrt{(1-\gamma)^2+4S}] \tag{18a}$$

where

$$\gamma=E_3/E_2. \tag{18b}$$

It is interesting to note that while the new perturbation series generated gives the correct bound at second order, third order becomes simply a scaled Langhoff–Davidson correction [27] for the unlinked terms arising out of the use of the variational principle. That is

$$W=\tilde{\varepsilon}_0+E_1+\frac{1}{\lambda}E_2 \tag{19a}$$

$$E_3(\lambda) = \frac{E_3}{\lambda^2} - \frac{E_2}{\lambda^2}[1-\lambda]$$

$$= \frac{1 \cdot E_2}{\lambda}(\lambda)[\gamma - 1 + \lambda]. \tag{19b}$$

We observe that Eq. (17) is the solution to the quadratic

$$\lambda^2 - \lambda(1-\gamma) - S = 0 \tag{20a}$$

$$\frac{S}{\lambda} = S(\lambda) = \gamma - 1 + \lambda. \tag{20b}$$

Hence substitution into Eq. (19b) yields the final scaled correction

$$E_3(\lambda) = \frac{1}{\lambda} \cdot E_2(\lambda) \cdot S(\lambda). \tag{21}$$

This scaled Langhoff–Davidson correction should approximately cancel the error caused by the unlinked clusters generated by Eq. (19a). If $E_3(\lambda)$ is added to Eq. (19a) for this purpose, then, of course, W is no longer necessarily an upper bound.

4. Perturbation Formulae to Fourth Order

The resulting perturbation or remainder of the Hamiltonian is defined for the Constant Denominator Perturbation Theory (CDPT) model as

$$V = H - H_0$$

$$= \sum_{pq} \langle p|M|q\rangle \eta[a_p^\dagger a_q] + \sum_{p>q} \sum_{r>s} \langle pq||rs\rangle \eta[a_p^\dagger a_q^\dagger a_s a_r] \tag{22a}$$

with indices p, q, r and s running over both the occupied and virtual space of spin orbitals. The monoelectronic operator, M, and the normal product, η, are defined respectively as

$$M = \sum_{p \neq q} \langle p|f|q\rangle \eta[a_p^\dagger a_q] + \sum_i \{\langle i|f|i\rangle - \bar{\varepsilon}\}\eta[a_i^\dagger a_i]$$

$$+ \sum_i \{\langle i^*|f|i^*\rangle - \bar{\varepsilon}^*\}\eta[a_{i^*}^\dagger a_{i^*}] \tag{22b}$$

$$\eta[a_1 a_2^\dagger a_3 a_4^\dagger a_5^\dagger \cdots a_n] = (-1)^p (a_2^\dagger a_4^\dagger a_5^\dagger \cdots a_1 a_3 \cdots a_n) \tag{22c}$$

where p is the parity of the permutation required to put all creation operators, $a_i^\dagger$, before any annihilation operators, a_j in Eq. (22c). The perturbation energy terms may be expressed in the symmetric form

$$E_{2n-1} = \langle \psi_n | E_0 - H_0 | \psi_{n-1}\rangle_L \tag{23a}$$

$$E_{2n} = \langle \psi_n | E_0 - H_0 | \psi_n\rangle_L \tag{23b}$$

$$|\psi_n\rangle = RV|\psi_{n-1}\rangle \tag{23c}$$

where the subscript L means that only linked diagrammatic representations are to be considered. The symmetric formulation and the rules for diagrammatic usage have been previously given in Refs. [21] and [22].

In the case of the first order wave function, ψ_1, the diagrammatic equations for single and double excitations are simply given by

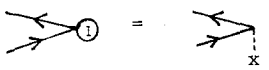

(24a)

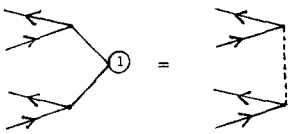

(24b)

where the open single arrows pointed to the left and right indicate individual particle and hole states respectively. The above equations are equivalent to

$$|\psi_{1_i}^{i^*}\rangle = \{i^*|j\}_1 |\Phi_j^{i^*}\rangle = \frac{\langle i^*|f|j\rangle}{\Delta\varepsilon} |\Phi_j^{i^*}\rangle \tag{25a}$$

$$|\psi_{1kl}^{i^*j^*}\rangle = \{i^*j^*||kl\}_1 |\Phi_{kl}^{i^*j^*}\rangle = \frac{\langle i^*j^*||kl\rangle}{2\Delta\varepsilon} |\Phi_{kl}^{i^*j^*}\rangle \tag{25b}$$

where the pseudo one and two electron matrix elements $\{i^*|j\}_1$ and $\{i^*j^*||kl\}_1$ are defined by their respective equations with

$$\langle i^*j^*||kl\rangle = \langle i^*j^*|kl\rangle - \langle i^*j^*|lk\rangle. \tag{25c}$$

The resulting diagrammatic equation for the second order energy is then given by

$E_2 =$ 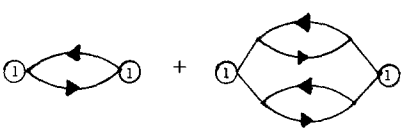

(26)

where the solid arrows are used to indicate summations over all possible particle and hole states. Using Eqs. (23) to (25) the above is re-expressed algebraically as

$$E_2 = \sum_{ij} \{j|i^*\}_1 \langle i^*|j\rangle_1 + \sum_{k>l} \sum_{i>j} \{kl||i^*j^*\}_1 \langle i^*j^*||kl\rangle_1 \tag{27a}$$

where the sums are over spin orbitals and

$$\langle i^*|j\rangle_1 = \Delta\varepsilon \{i^*|j\}_1 \tag{27b}$$

$$\langle i^*j^*||kl\rangle_1 = 2\Delta\varepsilon \{i^*j^*||kl\}_1 \tag{27c}$$

$$\{j|i^*\}_1 = \{i^*|j\}_1^\dagger \tag{27d}$$

$$\{kl||i^*j^*\}_1 = \{i^*j^*||kl\}_1^\dagger. \tag{27e}$$

In a similar fashion the single and double excitations of the second order wave function, ψ_2, that can be represented by connected diagrams are defined by the following equations

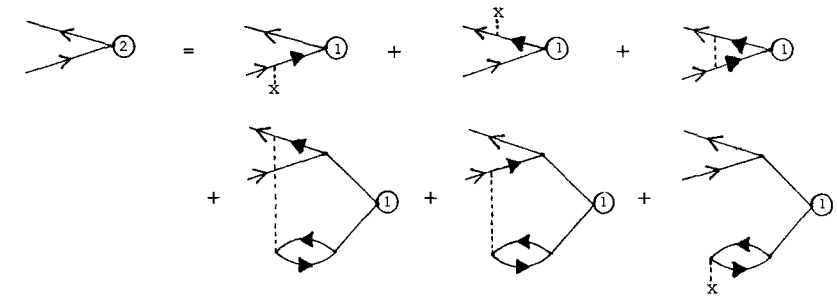

(28a)

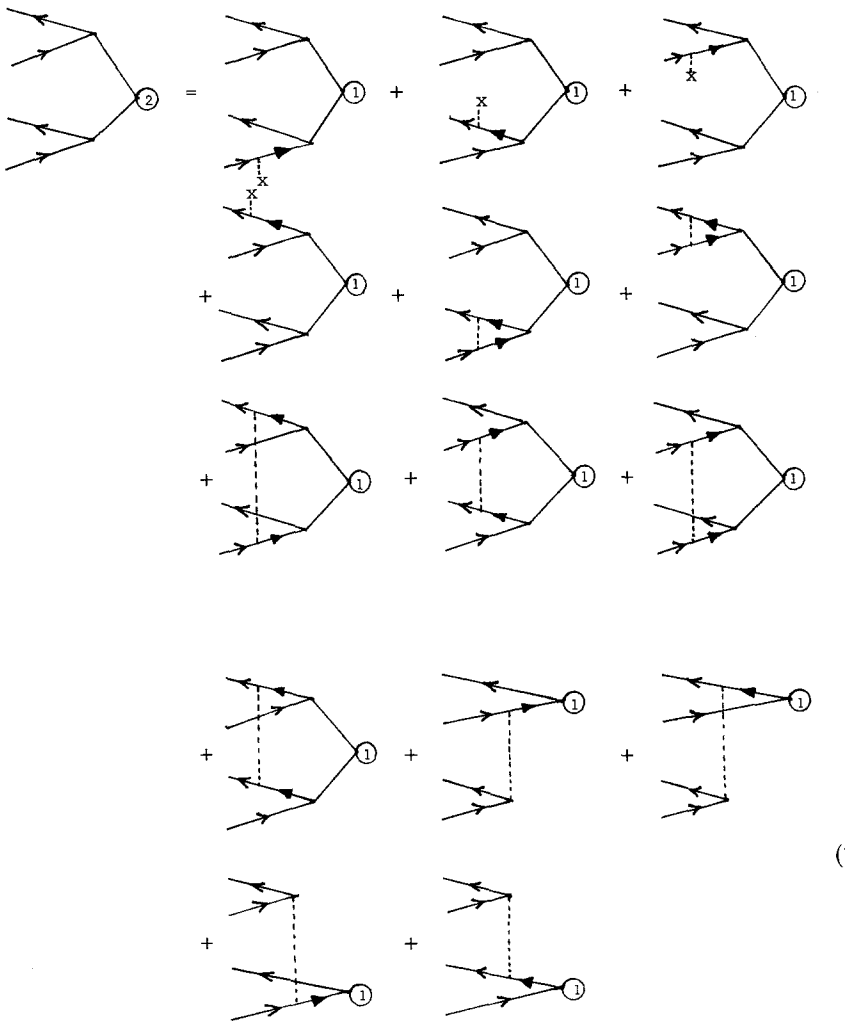

(28b)

where the solid arrows are used again to represent summations. In order to preserve the antisymmetry property of the bielectronic pseudo matrix elements all possible interactions on both open loops must be considered. Using the rules of diagrammatic perturbation theory, Eqs. (28a, b) can be re-expressed in algebraic form as

$$|\psi_{2_i}^{i^*}\rangle_C = \frac{\langle i^*|j\rangle_2}{\Delta\varepsilon}|\Phi_j^{i^*}\rangle = \{i^*|j\}_2|\Phi_j^{i^*}\rangle \tag{29a}$$

with

$$\begin{aligned}\langle i^*|j\rangle_2 = &\sum_k \langle k|M|j\rangle\{i^*|k\}_1 + \sum_k \langle i^*|M|k^*\rangle\{k^*|j\}_1 - \sum_{kl}\langle ki^*||jl^*\rangle\{l^*|k\}_1 \\ &+ \sum_m \sum_{k>l}\langle mi^*||k^*l^*\rangle\{k^*l^*||mj\}_1 - \sum_m\sum_{k>l}\langle kl||m^*j\rangle\{m^*i^*||kl\}_1 \\ &+ \sum_{kl}\langle k|M|l^*i^*\rangle\{l^*i^*||kj\}_1\end{aligned} \tag{29b}$$

and

$$|\psi_{kl}^{i^*j^*}\rangle_C = \frac{\langle i^*j^*||kl\rangle_2}{2\Delta\varepsilon}|\phi_{kl}^{i^*j^*}\rangle = \{i^*j^*||kl\}_2|\Phi_{kl}^{i^*j^*}\rangle \tag{29c}$$

with

$$\begin{aligned}\langle i^*j^*||kl\rangle_2 = &-\sum_m\langle k|M|m\rangle\{i^*j^*||ml\}_1 + \sum_m\langle m^*|M|i^*\rangle\{m^*j^*||kl\}_1 \\ &-\sum_m\langle l|M|m\rangle\{i^*j^*||km\}_1 + \sum_m\langle m^*|M|j^*\rangle\{i^*m^*||kl\}_1 \\ &-\sum_{mn}\langle mi^*||kn^*\rangle\{n^*j^*||ml\}_1 - \sum_{mn}\langle mj^*||ln^*\rangle\{i^*n^*||km\}_1 \\ &-\sum_{mn}\langle mj^*||kn^*\rangle\{i^*n^*||ml\}_1 - \sum_{mn}\langle i^*m||n^*l\rangle\{n^*j^*||km\}_1 \\ &+\sum_{m>n}\langle mn||kl\rangle\{i^*j^*||mn\}_1 + \sum_{m>n}\langle i^*j^*||m^*n^*\rangle\{m^*m^*||kl\}_1 \\ &-\sum_m\langle i^*m||kl\rangle\{j^*|m\}_1 + \sum_m\langle i^*j^*||km^*\rangle\{m^*|l\}_1 \\ &-\sum_m\langle mj^*||kl\rangle\{i^*|m\}_1 + \sum_m\langle i^*j^*||m^*l\rangle\{m^*|k\}_1.\end{aligned} \tag{29d}$$

As always, sums are over spin orbitals. The subscript, C, implies only connected types of diagrammatic excitations. In addition, triply connected diagrammatic excitations occur in ψ_2. These are formally generated from the diagrammatic

equation

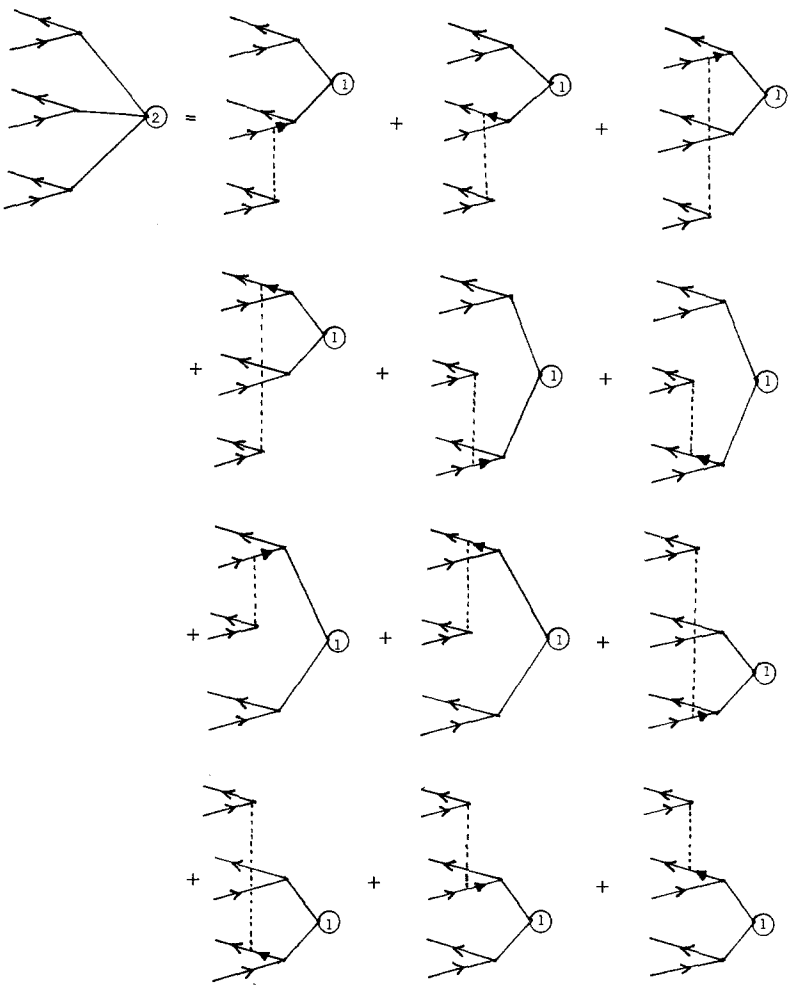

(30a)

where all possible interactions on all possible loops are considered so that the resulting compound matrix element $\{i^*j^*k^*|lmn\}_2$ is symmetric with respect to interchange of pairs of particle and hole lines. The compound matrix element is defined as [22]

$$|\psi_2^C\begin{pmatrix} i^* & j^* & k^* \\ l & m & n \end{pmatrix}) = \{i^*j^*k^*|lmn\}_2|\phi_{lmn}^{i^*j^*k^*}\rangle \tag{30b}$$

$$\{i^*j^*k^*|lmn\}_2 = \frac{\langle i^*j^*k^*|lmn\rangle_2}{3\Delta\varepsilon} \tag{30c}$$

$$\langle i^*j^*k^*|lmn\rangle_2 = \sum_P [-\langle i^*p||lm\rangle\{j^*k^*||pm\}_1 +$$

$$+\langle i^*j^*||lp^*\rangle\{p^*k^*||mn\}_1 - \langle i^*p||ln\rangle\{j^*k^*||mp\}_1 +$$

$$+\langle i^*k^*||lp^*\rangle\{j^*p^*||mn\}_1-\langle pj^*||lm\rangle\{i^*k^*||pn\}_1+$$
$$+\langle i^*j^*||p^*m\rangle\{p^*k^*||ln\}_1-\langle j^*p||mn\rangle\{i^*k^*||lp\}_1+$$
$$+\langle j^*k^*||mp^*\rangle\{i^*p^*||ln\}_1-\langle pk^*||ln\rangle\{i^*j^*||pm\}_1+$$
$$+\langle i^*k^*||p^*n\rangle\{p^*j^*||lm\}_1-\langle pk^*||mn\rangle\{i^*j^*||lp\}_1+$$
$$+\langle j^*k^*||p^*n\rangle\{i^*p^*||lm\}_1]. \tag{30d}$$

It can be seen that Eq. (30) is an N^7 step for *ab-initio* methods, although for semi-empirical schemes such as CNDO/2 and PPP the evaluation is N^3 in a basis of bonds and antibonds. However, unlike Nesbet–Epstein [10] or Moller–Plesset [9] partitioning schemes, there is no coupling of components through the denominators. It will be seen in the next section, that when the resulting energy diagrams arising from the connected triples are considered, all evaluation steps can be reduced to N^6 or less due to this decoupling.

In addition to the diagrammatically connected excitations, there is the possibility of independent single and double excitations occurring simultaneously in the system, resulting in net double, triple, or quadruple excitations. These excitations are represented by the following disconnected diagrams.

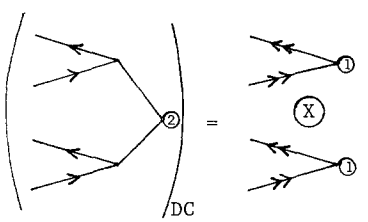

(31a)

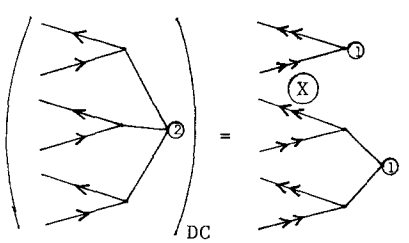

(31b)

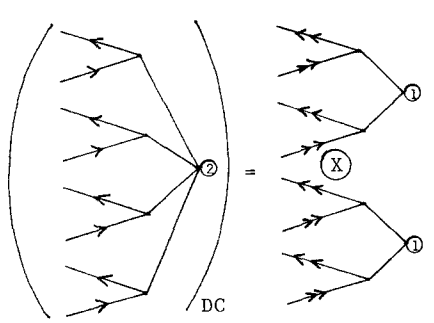

(31c)

where the subscript "*DC*" implies only disconnected diagrams are considered and double arrows are used to indicate that all possible combinations of indices which give rise to the same individual excitation are taken into account. From the factorization lemma [28], one knows that the product, ⊗, of the disconnected parts generates all possible (time) orderings that these components can have with each other; for example

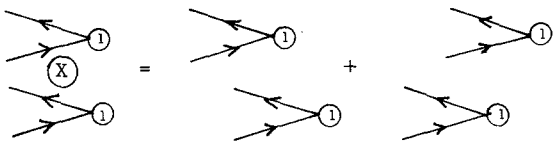

(32)

Since the resulting energy expansion will be expressed in terms of the individual connected parts of the wave function diagrams, be they connected or disconnected, it is unnecessary to consider the algebraic formulations of Eqs. (31). In addition, many of the resulting exclusion principle violating (EPV) energy diagrams are found to cancel against other contributions which are formally triple and quadruple excitations due to differences in their spin parts. This was previously demonstrated for the zero differential overlap (ZDO) case in Ref. [22]. Although we do not make formal use of this cancellation and let it occur naturally, we can for the *ab-initio* case develop a similar explicit cancellation using Goldstone diagrams.

From the first order wave function, ψ_1, of Eqs. (25), the second order energy, E_2, found from Eq. (23b) is given diagrammatically as Eq. (26). Similarly, the use of ψ_1 with the second order wave function, ψ_2, in Eq. (23a) leads to the diagrammatic Eq. for E_3, the third order energy.

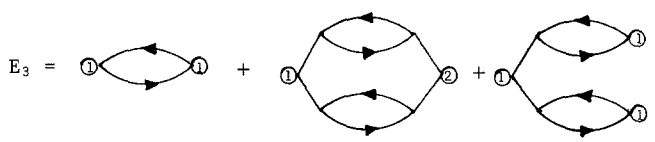

(33a)

where the disconnected double excitation found in the last term is generated from the product of two single excitations as previously discussed. The above yields the algebraic equation

$$E_3 = \sum_{ij} \{j|i^*\}_1 \langle i^*|j\rangle_2 + \sum_{i>j}\sum_{k>l} \{kl||i^*j^*\}_1 \{i^*j^*||kl\}_2$$

$$+ \sum_{i>j}\sum_{k>l} \langle kl||i^*j^*\rangle_1 [\{i^*|k\}_1 [\{j^*|l\}_1 - \{i^*|l\}_1 \{j^*|k\}_1] \tag{34b}$$

Finally, the fourth order energy, E_4 can also be diagrammatically generated from ψ_2 and Eq. (23b)

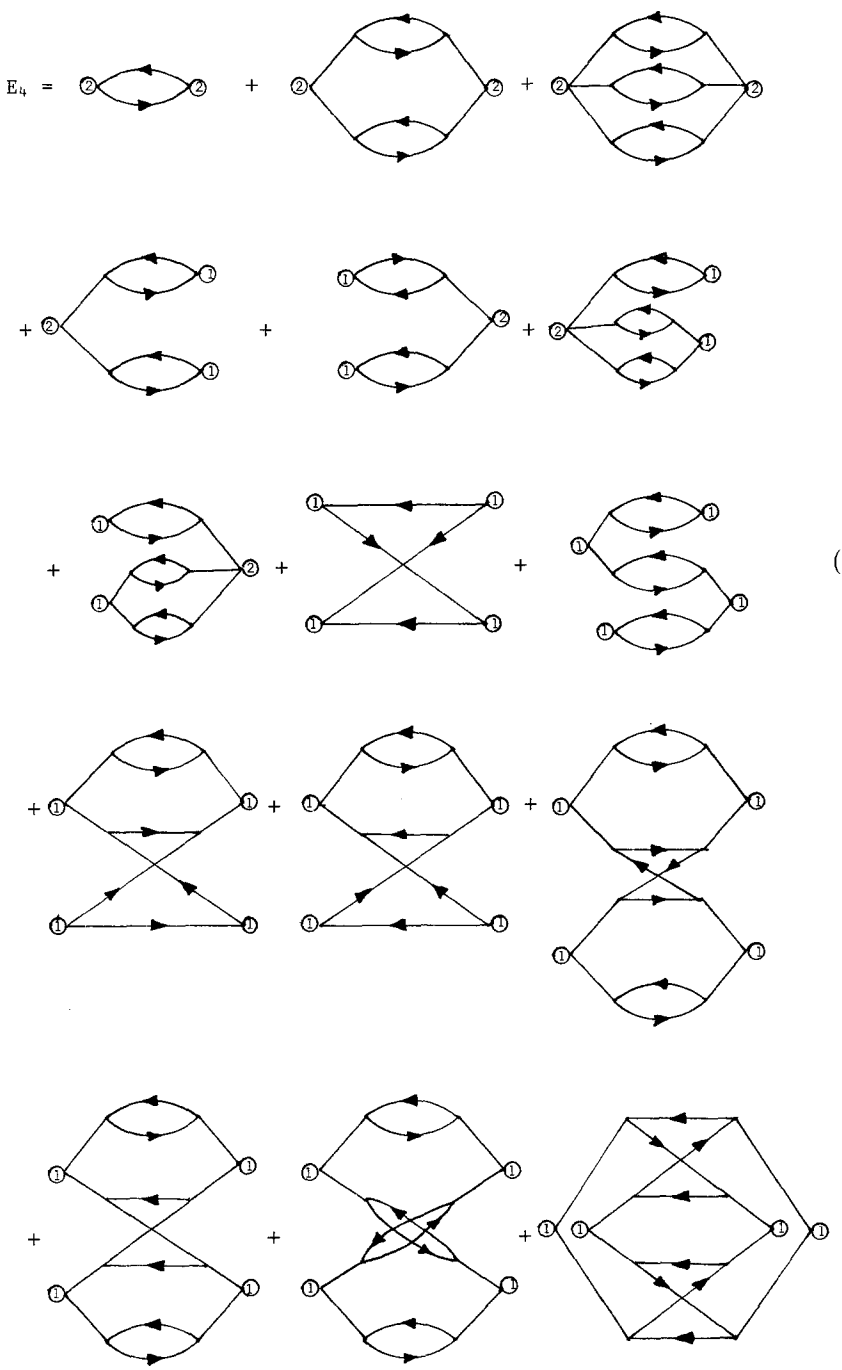

(35a)

where all possible topologically distinct orderings of the disconnected parts of the diagrams are taken. Thus algebraically one has

$$
\begin{aligned}
E_4 = & \sum_{ij} \{j|i^*\}_2 \langle i^*|j\rangle_2 + \sum_{i>j} \sum_{k>l} \{kl||i^*j^*\}_2 \langle i^*j^*||kl\rangle_2 \\
& + \sum_{i>j} \sum_{k>l} \sum_{m>n} \{lmn|i^*j^*k^*\}_2 \langle i^*j^*k^*|lmn\rangle_2 \\
& + 2 \sum_{i>j} \sum_{k>l} \langle kl||i^*j^*\rangle_2 [\{i^*|k\}_1 \{j^*|l\}_1 - \{i^*|l\}_1 \{j^*|k\}_1] \\
& + 2 \sum_{i>j} \sum_{l>m} \sum_{kn} \langle lmn|i^*j^*k^*\rangle_2 \{i^*j^*||lm\}_1 \{k^*|n\}_1 \\
& - \sum_{i>j} \sum_{k>l} \langle k|i^*\rangle_1 \{l|j^*\}_1 \{j^*|k\}_1 \{i^*|l\}_1 \\
& + \sum_{ijk} \sum_{lm} \sum_{n} [\langle lm||i^*j^*\rangle_1 \{n|k^*\}_1 + \{lm||i^*j^*\}_1 \langle n|k^*\rangle_1] \{i^*|l\}_1 \{j^*k^*||mn\}_1 \\
& - \sum_{l>m} \sum_{ijk} \sum_{n} [\langle lm||i^*j^*\rangle_1 \{n|k^*\}_1 + \{lm||i^*j^*\}_1 \langle n|k^*\rangle_1] \{i^*k^*||lm\}_1 \{j^*|n\}_1 \\
& - \sum_{i>j} \sum_{kl} \sum_{mn} [\langle lm||i^*j^*\rangle_1 \{n|k^*\}_1 + \{lm||i^*j^*\}_1 \langle n|k^*\rangle_1] \{i^*j^*||ln\}_1 \{k^*|m\}_1 \\
& - \sum_{ij} \sum_{kl} \sum_{m>n} \sum_{p>q} \langle i^*j^*||mn\rangle_1 \{k^*l^*||pq\}_1 \{i^*k^*||mn\}_1 \{j^*l^*||pq\}_1 \\
& - \sum_{i>j} \sum_{k>l} \sum_{mn} \sum_{pq} \langle i^*j^*||mn\rangle_1 \{k^*l^*||pq\}_1 \{i^*j^*||mp\}_1 \{k^*l^*||nq\}_1 \\
& - \sum_{ij} \sum_{kl} \sum_{mn} \sum_{pq} \langle i^*j^*||mn\rangle_1 \{k^*l^*||pq\}_1 \{i^*k^*||mp\}_1 \{j^*l^*||nq\}_1 \\
& + \sum_{i>j} \sum_{k>l} \sum_{mn} \sum_{pq} \langle i^*j^*||mn\rangle_1 \{k^*l^*||pq\}_1 \{i^*j^*||pq\}_1 \{k^*l^*||mn\}_1 \qquad (35b)
\end{aligned}
$$

where all matrix elements have been assumed real, so that for reversed ordered pairs of diagrams, such as

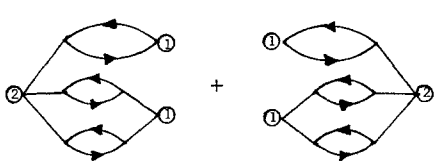

only the first member is considered and multiplied by a factor of two to include the contribution of the other partner.

5. The Energy Contributions of the Connected Triple Excitations

The contributions from the connected triple excitations are given by

$$E_4\begin{pmatrix}\text{Connected}\\ \text{Triples}\end{pmatrix} = E_4^{\text{CC-Triple}} + E_4^{\text{CD-Triple}} \tag{36a}$$

with

$$E_4^{\text{CC-Triple}} = \sum_{i>j>k}\sum_{l>m>n} \{lmn|i^*j^*k^*\}_2\langle i^*j^*k^*|lmn\rangle_2 \tag{36b}$$

$$E_4^{\text{CD-Triple}} = 2\sum_{i>j}\sum_{l>m}\sum_{kn}\langle lmn|i^*j^*k^*\rangle_2\{i^*j^*||lm\}_1\{k^*|n\}_1. \tag{36c}$$

Diagrammatically, the connected-connected triple excitation contribution, $E_4^{\text{CC-Triple}}$, is represented by

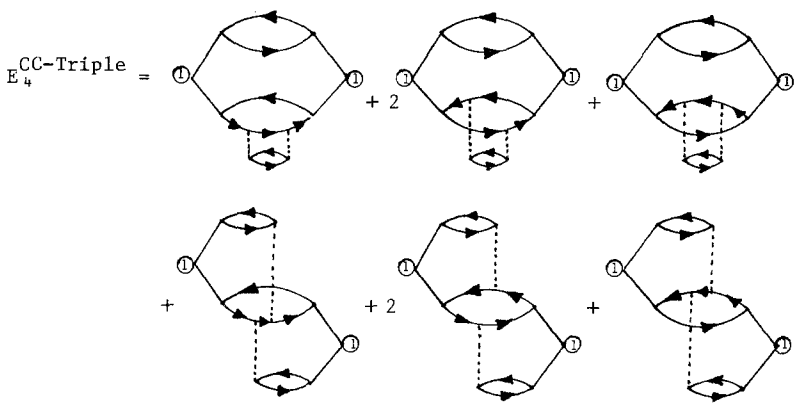

(37a)

or algebraically this yields

$$\begin{aligned}
E_4^{\text{CC-Triple}} = {} & \frac{1}{12\Delta}\sum_{pq}\left[\sum_{ilm}\langle lm||i^*q\rangle\langle i^*p||lm\rangle\right]\left[\sum_{jkn}\{qn||j^*k^*\}_1\{j^*k^*||pn\}_1\right] \\
& -\frac{2}{3\Delta}\sum_{pq}\sum_{jm}\left[\sum_{kn}\{mn||q^*k^*\}_1\{j^*k^*||pn\}_1\right]\left[\sum_{il}\langle lq^*||i^*j^*\rangle\langle i^*p||lm\rangle\right] \\
& +\frac{1}{12\Delta}\sum_{pq}\left[\sum_{ijl}\langle lq^*||i^*j^*\rangle\langle i^*j^*||lp^*\rangle\right] \\
& \times\left[\sum_{kmn}\{mn||q^*k^*\}_1\{p^*k^*||mn\}_1\right] \\
& +\frac{1}{3\Delta}\sum_{pq}\sum_{jm}\left[\sum_{kn}\{qn||j^*k^*\}_1\langle pk^*||mn\rangle\right]\left[\sum_{il}\langle ml||qi^*\rangle\{i^*j^*||lp\}_i\right] \\
& -\frac{2}{3\Delta}\sum_{pq}\left[\sum_{jkn}\{pn||j^*k^*\}_1\langle j^*k^*||q^*n\rangle\right]\left[\sum_{lmi}\langle lm||i^*p\rangle\{i^*q^*||lm\}_1\right]
\end{aligned}$$

$$+\frac{1}{3\Delta}\sum_{pq}\sum_{jm}\left[\sum_{kn}\{p^*k^*||mn\}_1\langle j^*k^*||q^*n\rangle\right]$$

$$\times\left[\sum_{il}\langle lp^*||i^*j^*\rangle\{i^*q^*||lm\}_1\right]. \tag{37b}$$

Similarly, the connected-disconnected triple excitation contribution, $E_4^{\text{CD-Triple}}$, is represented by

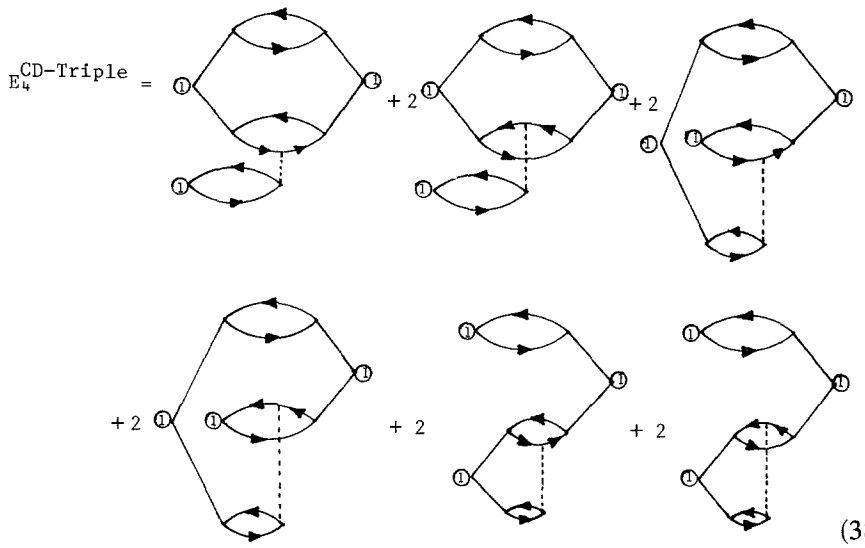

(38a)

In the above, all orderings of the disconnected components are implied from the factorization lemma [28]. The diagrams of Eq. (38a) are represented algebraically by

$$E_4^{\text{CD-Triple}} = -\sum_p\sum_m\left[\sum_{il}\{l|i^*\}_1\langle i^*p||lm\rangle\right]\left[\sum_{jkn}\{mn||j^*k^*\}_1\{j^*k^*||pn\}_1\right]$$

$$+\sum_q\sum_j\left[\sum_{il}\{l|i^*\}_1\langle i^*j^*||lq^*\rangle\right]\left[\sum_{mnk}\{mn||j^*k^*\}_1\{q^*k^*||mn\}_1\right]$$

$$-2\sum_p\sum_{ijl}\left[\sum_m\{m|j^*\}_1\langle i^*p||lm\rangle\right]\left[\sum_{kn}\{ln||i^*k^*\}_1\{j^*k^*||pn\}_1\right]$$

$$+2\sum_q\sum_{iml}\left[\sum_j\{m|j^*\}_1\langle i^*j^*||lq^*\rangle\right]\left[\sum_{kn}\{ln||i^*k^*\}_1\{q^*k^*||mn\}_1\right]$$

$$-2\sum_p\sum_j\left[\sum_{kn}\{n|k^*\}_1\{j^*k^*||pn\}_1\right]\left[\sum_{lmi}\{lm||i^*j^*\}_1\langle i^*p||lm>\right]$$

$$+2\sum_q\sum_m\left[\sum_{kn}\{n|k^*\}_1\{q^*k^*||mn\}_1\right]\left[\sum_{lij}\{lm||i^*j^*\}_1\langle i^*j^*||lq^*\rangle\right]. \tag{38b}$$

Table 2. Comparison of the various perturbation theories for the PPP model Hamiltonian[a]

Molecule	Hartree Fock	Constant denominator perturbation theory Second order	Third order	Fourth order	Rayleigh–Schrödinger perturbation theory Fourth order Moller–Plesset	Fourth order Nesbet–Epstein	CISD	Exact
Butadiene (M.N.)[c]	−0.742	−1.869	−2.214	−2.103	−2.015	−1.995	−2.039	−2.122[e]
Butadiene (O.K.)[d]	−0.668	−1.074	−1.199	−1.192	−1.069	−1.191	−1.211	−1.234[e]
Hexatriene (M.N.)	−1.526	−2.817	−3.551	−3.538	−3.372	−3.297	−3.157	−3.539[e]
Hexatriene (O.K.)	−1.368	−1.768	−2.091	−2.145	−1.921	−2.130	−2.086	−2.224[e]
Benzene (M.N., $\beta = -2.5$)	−4.702	−4.130	−5.970	−6.314	−5.677	−7.027	−5.186	−6.066[f]
Benzene (M.N., $\beta = -5.0$)	−9.702	−5.698	− 8.971	−10.416	−10.416	−11.155	−9.208	−10.369[f]
Benzene (M.N., $\beta = -10.0$)	−19.702	−12.999	−19.902	−22.017	−21.660	−22.513	−18.134	−20.040[f]
$C_{10}H_{10}$ (M.N., $\beta = -2.5$)	−6.347	−5.139	−7.273	−7.931	−7.867	−7.417	−6.443	−8.996[f]
$C_{10}H_{10}$ (M.N., $\beta = -5.0$)	−13.708	−7.877	−11.017	−12.223	−12.743	−12.587	−11.412	−14.978[f]
Relative error[b]		54	15	9[b]	11	11	16	

[a] All results are quoted in eV relative to $\langle \Phi_0 | H | \Phi_0 \rangle$

[b] Relative error $= 100 \left[\frac{(E_{\text{calc}} - E_{\text{exact}})^2}{E_{\text{exact}}^2 N - 1} \right]^{1/2}$ %

[c] M.N. ≡ Mataga–Nishimoto

[d] O.K. ≡ Ohno–Klopman

[e] Ref. [29]

[f] Ref. [30]

Table 3. Comparison of the various perturbation theories for the CNDO/2 model Hamiltonian[a]

Molecule	Hartree Fock	Constant denominator perturbation theory Second order	Third order	Fourth order	Rayleigh–Schrödinger perturbation theory Fourth order Moller-Plesset	Fourth order Nesbet-Epstein	CISD
CH_4	−1.28	−23.51	−24.09	−25.66	−23.72	−25.93	−25.02
C_2H_2	−12.66	−56.36	−58.95	−64.10	−63.64	−71.58	−61.16
C_2H_4	−36.24	−73.47	−78.94	−86.69	−83.68	−89.44	−83.37
C_2H_6	−35.14	−69.56	−75.60	−80.76	−76.58	−82.07	−77.31
CH_3CN[b]	−74.11	−118.70	−132.11	−150.46	−150.13	−172.26	−140.47
CH_3CN	−80.75	−122.10	−135.85	−154.91	−158.40	−158.18	−146.49
CH_3NC[b]	−54.61	−99.07	−107.83	−124.74	−126.77	−148.11	−117.69
CH_3NC	−220.66	−218.48	−250.14	−256.64	−310.22	−598.08	−267.39
H_2O[b]	−3.39	−18.03	−18.36	−20.44	−18.60	−22.59	−20.56
H_2O	−25.75	−38.54	−40.05	−41.10	−41.37	−53.64	−42.35
NH_3[b]	−4.28	−29.21	−30.15	−32.75	−30.25	−34.90	−32.27
NH_3	−13.39	−35.97	−37.37	−40.10	−39.53	−47.09	−40.94

[a] All energies are quoted in kcal/mole and are relative to E_0+E_1; [b] Optimized polarities

Thus it is seen that all contributions from connected triple excitations can be evaluated in steps that are at most N^6.

6. Results and Discussion

Results for the PPP model Hamiltonian are displayed in Table 2. The second order energy provides a useful bound; for the linear molecules this energy is below the Hartree–Fock energy. At fourth order the constant denominator theory seems superior to either Moller–Plesset or Nesbet–Epstein theories, and is very accurate in the linear cases. None of these theories are particularly good for the aromatic situations with pathologically large β values.

In Table 3 the CNDO/2 model Hamiltonian [31–35] results corroborate these findings. In particular the second order energy is a bound and in all cases (except CH_3NC: nonoptimized polarities (36)) is a better bound than the Hartree–Fock; as hoped for, much of the correlation present in the doubles is already included compared with CISD.

Comparing with the PPP results of Table 2 we might conclude that deficiencies at second order are arising in strongly delocalized systems, and that these deficiencies due to delocalization (single excitations) are not fully corrected at fourth order. The third order, however, on the average appears to be as accurate as CISD when compared with the exact results when known.

For small systems such as CH_4, NH_3, H_2O, where singles and doubles might be expected to contain most of the correlation, the fourth order results lie very close to the CISD, Table 3. In addition, the fourth order CDPT values lie between the MP and NE numbers. For larger systems CDPT is above fourth order MP or NE theories, and below CISD by an amount that might be considered reasonable.

The difference between optimized and nonoptimized polarities gives an indication of the behavior and convergence of the perturbation series. As one goes to higher orders this difference should approach zero. In the case of CH_3NC, the CDPT model reduces the difference between optimized and nonoptimized results of -166 kcal/mole at first order to -45 kcal/mole at second order and

Table 4. Energy differences obtained between a reference function of optimized *vs.* standardized bonds (kcal/mole)[a]

	$\varepsilon_0+\varepsilon$	Fourth Order CDPT	Fourth Order MPPT	Fourth Order NEPT	CISD
CH_3CN	−6.6	−2.2	1.6	6.3	−0.6
CH_3NC	−166.1	−34.2	17.4	283.9	−16.4
H_2O	−22.4	−1.7	0.4	8.7	−0.6
NH_3	−9.1	−1.7	0.2	3.1	−0.4

[a] 1 kcal/mol = 1.6 milli-Hartree

−324 kcal/mole at fourth order, to be compared with a 17 kcal/mole difference obtained from MP fourth order theory, a 284 kcal/mole difference obtained from the Nesbet-Epstein fourth order theory, and −16 kcal/mole for CISD, Table 4. Similarly, for H_2O the difference of −22.4 kcal/mole has been reduced to −1.7 kcal/mole and for NH_3 from −9.1 kcal/mole to −1.7 kcal/mole. In all cases most of this correction is already at second order. The indication here is that CDPT is nearly as accurate as is the more time-expensive fourth order MPPT and CISD in treating polarization, and much more accurate then NEPT which is very sensitive to the choice of zero'th order function.

Geometry predictions, Table 5, are as good as can be expected in the CNDO/2 treatment with essentially no difference in results between third and fourth order theories.

Table 5. Geometry predictions of constant denominator perturbation theory

Molecule	Bond distance or angle[a]	Third order result	Fourth order result	Experimental	Reference
CH_4	R_{CH}	1.124	1.125	1.085	[37]
H_2O[b]	R_{OH}	1.043	1.047	0.957	[38]
	θ(HOH)	104.5	102.6	104.5	
H_2O	R_{OH}	1.043	1.047	0.957	
	θ(HOH)	104.5	102.6	104.5	
NH_3[b] R_{NH}				1.012	[39]
	θ(HNH)			106.7	
NH_3	R_{NH}	1.078		1.012	
	θ(HNH)	106.6		1.067	
C_2H_2	R_{CC}	1.225	1.225	1.205	[40]
	R_{CH}	1.102	1.106	1.059	
H_2CO[b]	R_{CO}	1.273	1.256	1.210	[41]
	R_{CH}	1.112	1.125	1.128	
H_2CO	R_{CO}	1.273	1.256	1.210	
	R_{CH}	1.112	1.126	1.128	
C_2H_4	R_{CC}	1.335	1.337	1.336	[42]
	R_{CH}	1.118	1.121	1.103	
CH_3CN[b]	R_{CN}	1.208	1.215	1.15	[43]
	R_{CC}	1.460	1.459	1.460	
	R_{CH}	1.126	1.128	1.112	
CH_3CN	R_{CN}	1.208	1.215	1.15	
	R_{CC}	1.460	1.459	1.46	
	R_{CH}	1.127	1.130	1.112	
CH_3NC	R_{NC}	1.208	1.208	1.18	[43]
	R_{CN}	1.419	1.419	1.44	
	R_{CH}	1.119	1.119	1.09	
C_2H_6	R_{CC}	1.476	1.473	1.532	[44]
	R_{CH}	1.129	1.121	1.107	

[a] All bond distances are given in Angstroms and angles in degrees
[b] Optimized bond polarities

Tentatively we hold that the CDPT theory is the most stable of the fourth order theories we have examined. The Nesbet–Epstein theory at fourth order is very sensitive to the zero'th order function and can be unreliable. The Moller–Plesset perturbation theory (MPPT) at fourth order appears stable. For small systems, however, CDPT appears to lie closer to the exact answer where the numbers are available. From Table 3 fourth order Moller–Plesset also seems to correct for deficiencies in bond polarization of the zero'th order function. It is more difficult to evaluate the relative performance of CDPT *vs.* MPPT for larger systems where exact answers are not yet available. For such systems MPPT may have an advantage of being size consistent at all orders, whereas the variational procedure adapted at second order for CDPT introduces non-linked terms that yield stability, but that are not corrected for until higher orders. This deficiency, however, is not a consequence of the constant denominator perturbation theory, but only of our choice of constant denominator. Denominators can be chosen to yield a linked theory at all orders, and we are presently investigating such choices.

Acknowledgements. This work was supported in part through a Natural Science and Engineering Research Council (Canada) grant. Much of the computing was performed under the Special Computing Program at the University of Guelph and we wish to acknowledge this important contribution. We are also pleased to acknowledge discussions with and helpful suggestions by Dr. Jiri Cizek (Guelph-Waterloo) and Dr. Rodney Bartlett (University of Florida), and also extend thanks to Ms. Jane Lilly for preparing this unusually difficult manuscript.

References

1. Bartlett, R. J., Purvis, G. D.: Physica Scripta **21**, 255 (1980)
2. Redmon, L. T., Purvis, G. D., Bartlett, R. J.: J. Chem. Phys. **72**, 986 (1980)
3. Bartlett, R. J., Shavitt, I., Purvis, G. D.: J. Chem. Phys. **71**, 281 (1979)
4. Redmon, L. T., Purvis, G. D., Bartlett, R. J.: J. Am. Chem. Soc. **101**, 2856 (1979)
5. Adams, G. F., Bent, G. D., Purvis, G. D., Bartlett, R. J.: J. Chem. Phys. **71**, 3697 (1979)
6. Pople, J. A., Krishnan, R., Schlegel, H. B., Binkley, J. S.: Int. J. Quantum Chem. **14**, 545 (1978)
7. Krishnan, R., Pople, J. A.: Int. J. Quantum Chem. **14**, 91 (1978)
8. Kello, V., Urban, M.: Int. J. Quantum Chem. **18**, 1431 (1980)
9. Moller, C., Plesset, M. S.: Phys. Rev. **146**, 618 (1934)
10. Nesbet, P. S.: Phys. Rev. **28**, 695 (1926); Nesbet, R. K.: Proc. Roy. Soc. (London) **A230**, 312 (1955); Proc. Roy. Soc. (London) **A230**, 322 (1955).
11. Millie, Ph., Levy, B., Berthier, G.: in Localization and delocalization in quantum chemistry, Vol. L, Dordrecht, Holland: Reidel (1975)
12. Nesbet, R. K.: Adv. Chem. Phys. **9**, Interscience, New York (1965)
13. Sinanoglu, O.: Adv. Chem. Phys. **6**, Interscience, New York (1964)
14. Staemmler, V., Kutzelnigg, W.: Theor. Chim. Acta (Berl.) **7**, 67 (1967)
15. Kutzelnigg, W.: in Localization and delocalization in quantum chemistry: Dordrecht, Holland: Reidel (1975)
16. Wilhitte, D. L., Whitten, J. C.: J. Chem. Phys. **58**, 948 (1973)
17. Masson, A., Levy, B., Malrieu, J. P.: Theor. Chim. Acta (Berl.) **18**, 197 (1970)
18. Pariser, R., Parr, R. G.: J. Chem. Phys. **21**, 466, 767 (1953); Pople, J. A.: Trans. Faraday Soc. **49**, 1375 (1953)
19. Pople, J. A., Segal, G. A.: J. Chem. Phys. **44**, 3289 (1966)

20. Cullen, J. M.: An approximate perturbation and variational perturbation model for molecular energy, M.Sc. Thesis, Department of chemistry, University of Guelph (1976)
21. Cullen, J. M.: Diagrammatic methods for the rapid evaluation of molecular ground state energy and conformation, Ph.D. Thesis, Dept. of Chemistry, University of Guelph (1981)
22. Cullen, J. M., Zerner, M. C.: Int. J. Quantum Chem. in press
23. Kelly, H. P.: Phys. Rev. **131**, 684 (1963).
24. Bartlett, R. J., Silver, D. M.: in Quantum science, ed. Calais, J. L., Goscinski, O., Linderberg, J., Öhrn, Y.: New York: Plenum Press (1976)
25. Bartlett, R. J., Shavitt, J.: Chem. Phys. Letters **50**, 190 (1977)
26. Cizek, J.: J. Chem. Phys. **45**, 4526 (1966)
27. Langhoff, S. R., Davidson, E. R.: Int. J. Quantum Chem. **8**, 61 (1974)
28. Frantz, L. M., Mills, R. L.: Nucl. Phys. **5**, 16 (1960)
29. Ohmine, J., Karplus, M., Schulten, K.: J. Chem. Phys. **68**, 2298 (1978)
30. Boyle, M. J.: The unitary group approach to the many electron correlation problem, Ph.D. Thesis, Dept. of Applied Mathematics, University of Waterloo, Waterloo, Ontario, Canada (1979)
31. Diner, S., Malrieu, J. P., Claverie, P., Jordan, F.: Chem. Phys. Letters **2**, 319 (1968)
32. Diner, S., Malrieu, J. P., Claverie, P.: Theor. Chim. Acta (Berl.) **13**, 1 (1969)
33. Malrieu, J. P., Claverie, P., Diner, S.: Theor. Chim. Acta (Berl.) **13**, 18 (1969)
34. Diner, S., Malrieu, J. P., Jordan, F., Gilbert, M.: Theoret. Chim. Acta (Berl.) **15**, 100 (1969)
35. Jordan, F., Gilbert, M., Malrieu, J. P., Pincelli, U.: Theoret. Chim. Acta (Berl.) **15**, 211 (1969)
36. Polarities of the bonds may be optimized by minimizing the second order contribution from excitations of the $\phi_i \rightarrow \phi_{i^*}$ type through a variation of the angle α of (1), see Ref [20] and [21] and [31] to [35]
37. Bartell, L. S., Kuchitsu, K., Denvi, R. J.: J. Chem. Phys. **35**, 1211 (1961)
38. Benedict, W. S., Gailer, N., Plyler, E. K.: J. Chem. Phys. **24**, 1139 (1956)
39. Bennett, W. S., Plyler, E. K.: Can. J. Phys. **35**, 1235 (1957)
40. Calloman, J. F., Stoicheff, B. P.: Can. J. Phys. **35**, 373 (1957)
41. Lawrence, R. B., Stranderg, M. W. P.: Phys. Rev. **83**, 363 (1951)
42. Bartell, L. S., Roth, E. A., Hollowell, C. D., Kuchitsu, K., Young, J. E. Jr.: J. Chem. Phys. **42**, 2683 (1965)
43. In: Tables of interatomic distances and configuration in molecules and ions, Special Publication No. 11, Chem. Soc. (London) (1958)
44. Bartell, L. S., Higginbotham, H. K.: J. Chem. Phys. **42**, 851 (1965)

Received October 15, 1982